International Journal of Research in Engineering and Science (IJRES)
ISSN (Online): 2320-9364, ISSN (Print): 2320-9356
www.ijres.org Volume 10 Issue 6 ǁ 2022 ǁ PP. 1905-1924

Effects of Soret-Dufour and radiation absorption with viscous dissipation on an unsteady MHD Casson Fluid Flow past a vertical plate through porous medium

A.K. Shukla[1], Shubham Kumar D[2], Mohammad Suleman Quraishi[3]
[1]Department of Mathematics RSKD PG College, U.P., India.
[2]Department of Mathematics RSKD PG College, U.P., India.
[3]Department of Applied Sciences, Jahangirabad Institute of Technology, U.P., India

Abstract
In this research article, we have analyzed the study of Casson fluid model with viscous dissipation, Soret-Dufour effect and radiation absorption on unsteady MHD Casson fluid flow past a vertical plate embedded in porous medium in the existence of radiation with heat generation/absorption. Governing equations of flow filed have been non-dimensionalizedfor this study , and have been solved numerically using the Crank-Nicolson implicit finite difference method. The effects of non-dimensional parameters on Concentration, temperature and velocity profiles are studied with the help of graphs and tables. Furthermore, parameters like skinfriction, Nusselt number and Sherwood number at dependency of various parameters are inspected through tables.

Keywords: *Casson Fluid, Viscous dissipation, Magnetohydrodynamics, Order of chemical reaction, Soret and Dufour effects, radiation effect.*

Date of Submission: 15-06-2022 Date of acceptance: 30-06-2022

I. INTRODUCTION

From many decades, alarge number of studies of applications of Non-Newtonian fluid flow filed in the presence of different effects due to this many mathematicians have takentheir great attention. Casson fluid is one of type of non-Newtonian fluid that reveals elasticity in nature, some examples of Casson fluid are honey, jelly, tomato sauce etc.. Human blood can also be treated as Casson fluid. Liaquat Ali Lund et al.[1] is investigated the magnetohydrodynamic (MHD) flow of Casson nanofluid with thermal radiation over an unsteady shrinking surface. Shahanaz Parvin et al.[2] are discussed effects of the mixed convection parameter, concentration buoyancy ratio parameter, Soret–Dufour parameters, and shrinking parameter in MHD Casson fluid flow past shrinking sheet. Lahmar et al.[3] studied heat transfer of squeezing unsteady nanofluid flow under the effects of an inclined magnetic field and variable thermal conductivity. Mohamed R.Eid et al. [4] investigated numerically for Carreau nanofluid flow over a convectively heated nonlinear stretching surface with chemically reactive species. Hammad Alotaibi et al.[5] introduced the effect of heat absorption (generation) and suction (injection) on magnetohydrodynamic (MHD) boundary-layer flow of Casson nanofluid (CNF) via a non-linear stretching surface with the viscous dissipation in two dimensions. Asogwa and Ibe [6] investigated numerical approach of MHD Casson fluid flow over a permeable stretching sheet with heat and mass transfer taking into cognizance the various parameters present. Renu et al.[7] assessed the effect of the inclined outer velocity on heat and flow transportation in boundary layer Casson fluid over a stretching sheet. Ramudu et al. [8] highlighted the impact of magnetohydrodynamic Casson fluid flow across a convective surface with cross diffusion, chemical reaction, non-linear radiative heat. Recently Mahabaleshwar et al.[9] discussed the important roles of SWCNTs and MWCNTs under the effect of magnetohydrodynamics nanofluids flow past over the stretching/shrinking sheet under the repercussions of thermal radiation and Newtonian heating. Ram Prakash Sharma et al. [10] reports MHD Non-Newtonian Fluid Flow past a Stretching Sheet under the Influence of Non-linear Radiation and Viscous Dissipation. Naveed Akbar et al.[11] investigated Numerical Solution of Casson Fluid Flow under Viscous Dissipation and Radiation Phenomenon. Elham Alali et al. [12] studied MHD dissipative Casson nanofluid liquid film flow due to an unsteady stretching sheet with radiation influence and slip velocity phenomenon. T. M. Ajayi et al. [13] have studied Viscous Dissipation Effects on the Motion of Casson Fluid over an Upper Horizontal Thermally Stratified Melting Surface of a Paraboloid of Revolution: Boundary Layer Analysis. N. Pandya and A. K. Shukla [14] have analyzed Effects of Thermophoresis, Dufour, Hall and Radiation on an Unsteady MHD flow past an Inclined Plate with Viscous Dissipation.

In this investigation our aim is to bring to light the effect of unsteady MHD Casson fluid flow through a vertical porous plate with Soret-Dufour, radiation absorption, heat source/sink and higher-order chemical reaction. The influence of various physical parameters on velocity, temperature and concentration profiles is discussed with the help of tables and graphs. On the other hand important physical quantities like shearing stress, Nusselt number and Sherwood number are discussed through tables.

II. MATHEMATICAL MODELING

The unsteady MHD Casson flow of a viscous incompressible electrically conductingfluid past an impulsively started infinite inclined porous plate with variable temperature and mass dispersal in the presence of radiation with viscous dissipation has been considered. The plate is vertical and is embedded in porous medium. The x- axis is taken along the plate and y-axis is taken normal to it. Initially, it is also assumed that the radiation heat flux in x- direction is negligible as compared to that in y -direction. The plate and fluid are at the same temperature and concentration. At time t, the plate is given some impulsive motion along x-direction against gravitational field with constant velocity u_0 , the plate temperature and concentration decrease exponentially with time. The transversely applied magnetic field and magnetic Reynolds number are very small and hence induced magnetic field is minute so it can be considered negligible, Cowling [16]. Due to infinite length in x-direction, the flow variables are functions of y and t only. Under the usual Boussinesq's approximation, governing partial differential equations for this unsteady flow field problem are given by:

2.1 Continuity equation:

$$\frac{\partial \bar{v}}{\partial \bar{y}} = 0 \quad \Rightarrow \bar{v} = -v_0 (constant) \tag{1}$$

2.2 Momentum equation:

$$\frac{\partial \bar{u}}{\partial \bar{t}} + \bar{v}\frac{\partial \bar{u}}{\partial \bar{y}} = \nu\left(1+\frac{1}{\beta}\right)\frac{\partial^2 \bar{u}}{\partial \bar{y}^2} + g\beta_t(\bar{T}-\bar{T}_\infty) + g\beta_c(\bar{C}-\bar{C}_\infty) - \frac{\sigma B_0{}^2 \bar{u}}{\rho} - \frac{\mu \bar{u}}{\rho_\infty \bar{K}} \tag{2}$$

2.3 Energy equation:

$$\rho_\infty C_p\left(\frac{\partial \bar{T}}{\partial \bar{t}} + \bar{v}\frac{\partial \bar{T}}{\partial \bar{y}}\right) = k\frac{\partial^2 \bar{T}}{\partial \bar{y}^2} - \frac{\partial q_r}{\partial \bar{y}} + \frac{\rho D_m K_T}{c_s}\frac{\partial^2 \bar{C}}{\partial \bar{y}^2} + \nu\left(1+\frac{1}{\beta}\right)\left(\frac{\partial \bar{u}}{\partial \bar{y}}\right)^2 - \bar{Q}_0\left(\bar{T}-\bar{T}_\infty\right) + Q_1\left(\bar{C}-\bar{C}_\infty\right) \tag{3}$$

$$\frac{\partial \bar{C}}{\partial \bar{t}} + \bar{v}\frac{\partial \bar{C}}{\partial \bar{y}} = D\frac{\partial^2 \bar{C}}{\partial \bar{y}^2} + \frac{D_m K_T}{T_m}\frac{\partial^2 \bar{T}}{\partial \bar{y}^2} - k_r\left(\bar{C}-\bar{C}_\infty\right)^n \tag{4}$$

$k_r\left(\bar{C}-\bar{C}_\infty\right)^n$	terms in mass equation for higher order chemical reaction
n	order of chemical reaction
k_r	chemical reaction constant
$\bar{C}$	concentration
$\bar{T}$	temperature
$\bar{T}_\infty$	temperature of free stream
$\bar{C}_\infty$	concentration of free stream
β	Casson parameter
βc	coefficient of volume expansion for mass transfer
β_t	volumetric coefficient of thermal expansion
T_m	mean fluid temperature
q_r	radiative heat along y ∗ -axis

$\overline{Q}_0$	Coefficient of heat source/sink
$\overline{Q}_1$	Radiation absorption parameter
ν	kinematic viscosity
$\overline{K}$	coefficient of permeability of porous medium
D_m	molecular diffusivity
k	thermal conductivity of fluid
c_p	specific heat at constant pressure
μ	viscosity
ρ	fluid density
σ	electrical conductivity
g	acceleration due to gravity
K_T	thermal diffusion ratio

In equation 4; $k_r\left(\overline{C}-\overline{C}_\infty\right)^n$ has come on account of nth order chemical reaction.
The boundary conditions for this model are assumed as:

$$\left.\begin{array}{llll} \bar{t}\le 0; & \bar{u}=0,\quad v_0=-v_0 & \overline{T}=\overline{T}_\infty,\quad \overline{C}=\overline{C}_\infty & \forall\,\bar{y} \\ \bar{t}>0; & \bar{u}=u_0, & \overline{T}=\overline{T}_\infty+(\overline{T}_w-\overline{T}_\infty)e^{-At},\ \ \overline{C}=\overline{C}_\infty+(\overline{C}_w-\overline{C}_\infty)e^{-At} & at\ \bar{y}=0 \\ & \bar{u}\to 0, & \overline{T}\to\overline{T}_\infty,\qquad \overline{C}\to\overline{C}_\infty \qquad as & \bar{y}\to\infty \end{array}\right\}\quad (5)$$

Where $A=\dfrac{V_0^{\ 2}}{\nu}$

Roseland explained the term radiative heat flux approximately as

$$q_r=-\frac{4\sigma_{st}}{3a_m}\frac{\partial\overline{T}^4}{\partial\bar{y}^4}\qquad (6)$$

Here Stefan Boltzmann constant and absorption coefficient are σ_{st} and a_m respectively.

In this case temperature differences are very-very small within flow, such that $\overline{T}^4$ can be expressed linearly with temperature. It is realized by expanding in a Taylor series about T_∞' and neglecting higher order terms, so

$$\overline{T}^4 \sim= 4\overline{T}_\infty^{\ 3}\overline{T}-3\overline{T}_\infty^{\ 4}\qquad (7)$$

With the help of equations (6) and (7), we write the equation (3) in this way

$$\left.\begin{array}{l} \rho_\infty C_p\left(\dfrac{\partial\overline{T}}{\partial\bar{t}}+\bar{v}\dfrac{\partial\overline{T}}{\partial\bar{y}}\right)=k\dfrac{\partial^2\overline{T}}{\partial\bar{y}^2}+\dfrac{16\overline{T}_\infty^{\ 3}\sigma_{st}}{3a_m}\dfrac{\partial^2\overline{T}}{\partial\bar{y}^2}+\dfrac{\rho D_m K_T}{c_s}\dfrac{\partial^2\overline{C}}{\partial\bar{y}^2} \\ +\nu\left(1+\dfrac{1}{\beta}\right)\left(\dfrac{\partial\bar{u}}{\partial\bar{y}}\right)^2-\overline{Q}_0\left(\overline{T}-\overline{T}_\infty\right)+Q_1\left(\overline{C}-\overline{C}_\infty\right) \end{array}\right\}\quad (8)$$

Let us introduce the following dimensionless quantities

$$\left.\begin{aligned}
&u=\frac{\bar{u}}{u_0},t=\frac{\bar{t}{v_0}^2}{\nu},y=\frac{\bar{y}v_0}{\nu},\ \theta=\frac{\overline{T}-\overline{T}_\infty}{\overline{T}_w-\overline{T}_\infty},C=\frac{\overline{C}-\overline{C}_\infty}{\overline{C}_w-\overline{C}_\infty},\\
&G_m=\frac{\nu g\beta_c(\overline{C}_w-\overline{C}_\infty)}{u_0{v_0}^2},G_r=\frac{\nu\, g\beta(\overline{T}_w-\overline{T}_\infty)}{u_0{v_0}^2},K=\frac{{v_0}^2}{\nu^2}\overline{K},\\
&S_c=\frac{\nu}{D},\ P_r=\frac{\mu C_p}{k},\ M=\frac{\sigma {B_0}^2\nu}{\rho {v_0}^2},R=\frac{4\sigma {\overline{T}_\infty}^3}{k_m k},K_r=\frac{k_r\,\nu}{{v_0}^2},\\
&Q=\frac{Q_0\nu}{\rho c_p {v_0}^2},D_u=\frac{D_mK_T(\overline{C}_w-\overline{C}_\infty)}{c_sc_p\nu(\overline{T}_w-\overline{T}_\infty)},S_r=\frac{D_mK_T(\overline{T}_w-\overline{T}_\infty)}{T_m\nu(\overline{C}_w-\overline{C}_\infty)},\\
&\qquad\overline{Q}\\
&Q_C=\frac{Q_1\nu(\overline{C}-\overline{C}_\infty)}{\rho c_p {v_0}^2(\overline{T}_w-\overline{T}_\infty)},Ec=\frac{{v_0}^2}{c_p(\overline{T}_w-\overline{T}_\infty)},A=\frac{{v_0}^2}{\nu}
\end{aligned}\right\}\tag{9}$$

Using substitutions of Equation 9, we get non-dimensional form of partial differential Equations 2, 8 and 4 respectively

$$\frac{\partial u}{\partial t}-\frac{\partial u}{\partial y}=\left(1+\frac{1}{\beta}\right)\frac{\partial^2 u}{\partial y^2}+G_r\theta+G_mC-\left(M+\frac{1}{K}\right)u\tag{10}$$

$$\frac{\partial\theta}{\partial t}-\frac{\partial\theta}{\partial y}=\frac{1}{P_r}\left(1+\frac{4R}{3}\right)\frac{\partial^2\theta}{\partial y^2}+D_u\frac{\partial^2C}{\partial y^2}+Ec\left(\frac{\partial u}{\partial y}\right)^2-Q\theta-Q_CC\tag{11}$$

$$\frac{\partial C}{\partial t}-\frac{\partial C}{\partial y}=\frac{1}{S_c}\frac{\partial^2C}{\partial y^2}+S_r\frac{\partial^2\theta}{\partial y^2}-K_rC^n\tag{12}$$

With initial and boundary conditions

$$\left.\begin{array}{lllll}
t\le 0; & u=0, & \theta=0, & C=0 & \forall y\\
t>0; & u=1, & \theta=e^{-t}, & C=e^{-t} & at\ y=0\\
u\to 0, & \theta\to 0, & C\to 0 & & as\ \ y\to\infty
\end{array}\right\}\tag{13}$$

The degree of practical attention include the Skin friction coefficients τ , local Nusselt Nu, and local Sherwood Sh numbers are known as follows:

$$\tau=-\left(1+\frac{1}{\beta}\right)\left(\frac{\partial u}{\partial y}\right)_{y=0},\ N_u=-\left(\frac{\partial\theta}{\partial y}\right)_{y=0},\ Sh=-\left(\frac{\partial C}{\partial y}\right)_{y=0}\tag{14}$$

III. Numerical Method of Solution

Exact solution of system of partial differential Equations 10, 11 and 12 with boundary conditions given by Equation 13 are impossible. So, these equations we have solved by Crank-Nicolson implicit finite difference method. The Crank-Nicolson finite difference implicit method is a second order method in time (o(Δt^2)) and space,hence no restriction on space and time steps, that is, the method is unconditionally stable. The computation is executed for $\Delta y = 0.1$, $\Delta t = 0.001$ and procedure is repeated till y = 4. Equations 10, 11 and 12 are expressed as

$$\frac{u_{i,j+1}-u_{i,j}}{\Delta t}-\frac{u_{i+1,j}-u_{i,j}}{\Delta y}=\left(1+\frac{1}{\beta}\right)\frac{u_{i-1,j}-2u_{i,j}+u_{i+1,j}+u_{i-1,j+1}-2u_{i,j+1}+u_{i+1,j+1}}{2(\Delta y)^2}$$

(15)

$$+G_r\left(\frac{\theta_{i,j+1}+\theta_{i,j}}{2}\right)+G_m\left(\frac{C_{i,j+1}+C_{i,j}}{2}\right)-M\left(1+\frac{1}{K}\right)\left(\frac{u_{i,j+1}+u_{i,j}}{2}\right)$$

$$\frac{\theta_{i,j+1}-\theta_{i,j}}{\Delta t}-\frac{\theta_{i+1,j}-\theta_{i,j}}{\Delta y}=\frac{1}{P_r}\left(1+\frac{4R}{3}\right)\left(\frac{\theta_{i-1,j}-2\theta_{i,j}+\theta_{i+1,j}+\theta_{i-1,j+1}-2\theta_{i,j+1}+\theta_{i+1,j+1}}{2(\Delta y)^2}\right)$$

$$+D_u\left(\frac{C_{i-1,j}-2C_{i,j}+C_{i+1,j}+C_{i-1,j+1}-2C_{i,j+1}+C_{i+1,j+1}}{2(\Delta y)^2}\right)+E_c\left(\frac{u_{i+1,j}-u_{i,j}}{\Delta y}\right)^2-Q\left(\frac{\theta_{i,j+1}+\theta_{i,j}}{2}\right)$$

$$-Q_c\left(\frac{C_{i,j+1}+C_{i,j}}{2}\right)$$

(16)

$$\frac{C_{i,j+1}-C_{i,j}}{\Delta t}-\frac{C_{i+1,j}-C_{i,j}}{\Delta y}=\frac{1}{S_c}\left(\frac{C_{i-1,j}-2C_{i,j}+C_{i+1,j}+C_{i-1,j+1}-2C_{i,j+1}+C_{i+1,j+1}}{2(\Delta y)^2}\right)$$

(17)

$$+S_r\left(\frac{\theta_{i-1,j}-2\theta_{i,j}+\theta_{i+1,j}+\theta_{i-1,j+1}-2\theta_{i,j+1}+\theta_{i+1,j+1}}{2(\Delta y)^2}\right)+K_r\left(\frac{C_{i,j+1}+C_{i,j}}{2}\right)^n$$

Initial and boundary conditions are also rewritten as:

$$u_{i,0}=0,\quad \theta_{i,0}=0,\quad C_{i,0}=0\qquad \forall i$$

$$u_{0,j}=1,\quad \theta_{0,j}=e^{-j\Delta t},\qquad C_{0,j}=e^{-j\Delta t}\qquad \forall j$$

(18)

$$u_{l,j}\to 0,\quad \theta_{l,j}\to 0,\quad C_{l,j}\to 0$$

Where index i represents to y and j represents to time t, $\Delta t = tj+1-tj$ and $\Delta y = yi+1-yi$. Getting the values of u, θ and C at time t, we may compute the values at time t+Δt as following method: we substitute i = 1, 2, ..., l−1 , where n correspond to ∞ ,equations 15 to 17 give tridiagonal system of equations with boundary conditions in equation 18, are solved employing Thomas algorithm as discussed in Carnahan et al.[15], we find values of θ and C for all values of y at t + Δt. Equation 15 is solved by same to substitute these values of θ and C, we get solution for u till desired time t.

IV. ANALYSIS OF RESULTS

The present work analyzes the boundary layer unsteady MHD Casson flow past a porous vertical plate with the Soret-Dufour effect. The influence of the order of chemical reaction has been incorporated in the mass equation. In order to see a physical view of work, numerical results of velocity profile u, temperature profile θ, concentration profile C have been discussed with the help of graphs and skin friction coefficients, Nusselt number and Sherwood number are discussed with the help of tables. The following values are used for investigation $Gr = 4$, $Gm = 7$ and $K = 1.2$, $M=3$, $\beta= 0.3$. It is noted from figure 2 that increasing radiation parameter R, velocity u increases. This is correct observation because the increase in radiation reveals heat energy to flow. In figure 5, velocity decreases as Prandtl number Pr increases and temperature decreases in figure 10 when Pr increases. In figure 22 concentration C near to plate decreases and some distance from plate concentration increases as Prandtl number increases. Figure 16 depicts the importance of radiation on temperature distribution. It is analyzed that an increase in R, temperature θ increases and it is notable that an increase in R, concentration C near to plate decrease after that increases in figure 19. Figure 18 depicts the variation of Schmidt number Sc as concentration decreases rapidly with increase Sc. It is noteworthy that on increasing Schmidt numbers Sc temperature profile in figure13 increases near to plate only while velocity profile in figure 9 decreases near to plate. In figure 8, 15 and 25, it is seen that velocity increases and concentration decreases as increase Dufour number Du, whereas temperature increases as Du increases. Figures 6 and 23 depict the behavior of chemical reaction parameter Kr on velocity and concentration respectively. It is seen that velocity decreases, concentration decreases rapidly as Kr increase. The negative value of $Q < 0$ means heat absorption and the positive value of $Q > 0$ means heat transfer. In figure 3, velocity profile decreases on increasing heat source/sink parameter Q and also reducing momentum boundary layer. Figure 12 analyzed the impact of heat source/sink parameter Q in the temperature profile. It can be seen that the temperature profile decreases rapidly and the thermal boundary layer reduces for an increase of heat source parameter but it increases with the heat sink parameter. Figure 21, depicts that concentration profile increases near to plate from middle of boundary layer it decreases as well as species boundary layer reduces on an increase of heat source/sink parameter. The influence of Radiation absorption parameter Q_c on the velocity, temperatureand concentration profiles in figure 4, 11 and figure 20 have been shown. We observe that when an increase Q_c results in the concentration profile also decreases while velocity andtemperature increases. Figure 1, 17 and 26 reveals that velocity, temperature and concentration increase on increase of time. Figure 7, 14 and 24 described that increment in Ec results in velocity and temperature increases and concentration decreses.

It is observed from **Table 1** that Change in Schmidt number Sc effects as skin friction coefficient and Sherwood number increases while Nusselt number decreases. Pr effects as skin friction coefficient and Nusselt number increases while Sherwood number decreases.Skin friction coefficient and Nusselt numberdecrease whereas Sherwood number increases with Dufour number Du increases and radiation parameter R increase. Increase in Soret number Sr, and Nusselt number Nu and Sherwood number increase while Skin friction decreases. On increasing Casson fluid parameter β results in skin friction decreases. It is also noted that increment in Q heat source/sink the skin friction coefficient and Sherwood number increases while Nusselt number decreases. Skin friction coefficient and Sherwood number decrease whereas Nusselt number increases when Qc heat absorption parameter increase. Increase in Eckert number affects the increment in Skin friction and Sherwood number while Nusselt number decreases.

V. CONCLUSION

Effect of second-order chemical reaction, change in Soret-Dufour on unsteady MHD flow past a vertical porous plate immersed in a porous medium are analyzed. This investigation the following conclusions have come:

5.1 The effect of radiation on concentration is noteworthy. It is observed that increasing values of R, concentration falls down and after some distance from the plate, it goes up slowly-slowly. Interestingly, the same type of change in concentration has been found on increasing Prandtl number P r.

5.2 For increasing values of Kr, it is a considerable enhancement in velocity, i.e. velocity decreases slowly.

5.3 Increasing values of Dufour number, it is observed that velocity and temperature profile in the thermal boundary layer increases whereas concentration profile first decreases after then increases slowly in the boundary layer.

5.4 Schmidt number greatly influences the concentration profile in the concentration boundary layer.

5.5 On increment in Eckert number Ec velocity and temperature increases and concentration decreases.

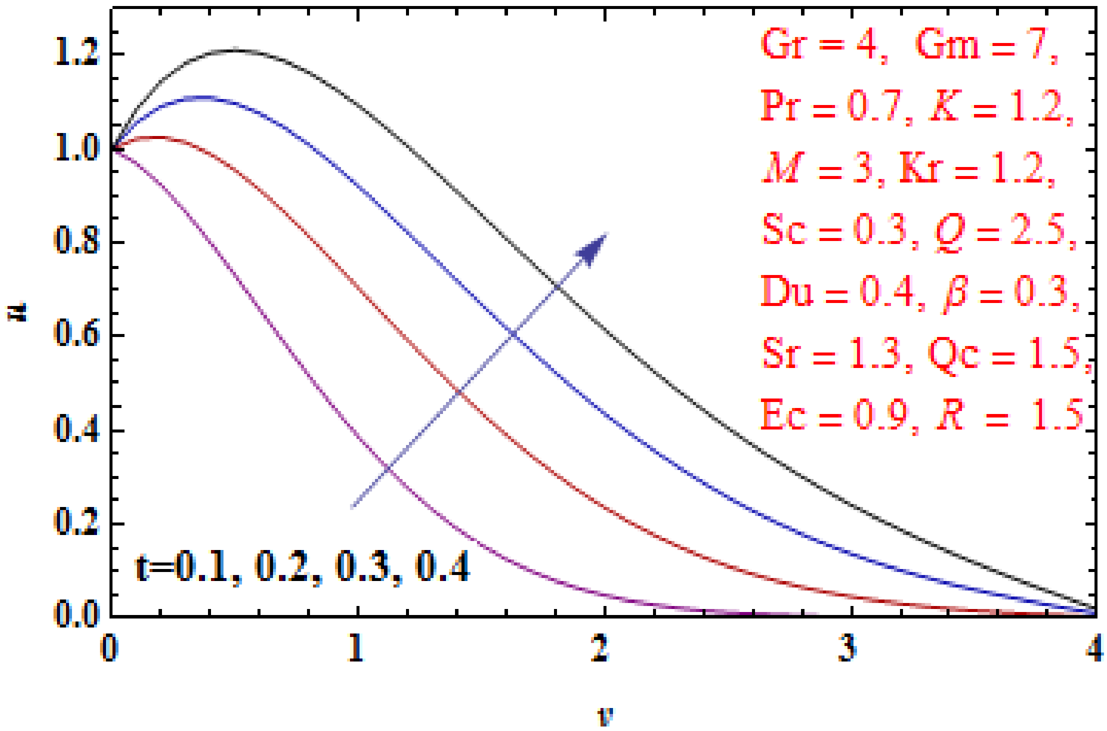

Figure. 1 Velocity Profiles for Different Values of t

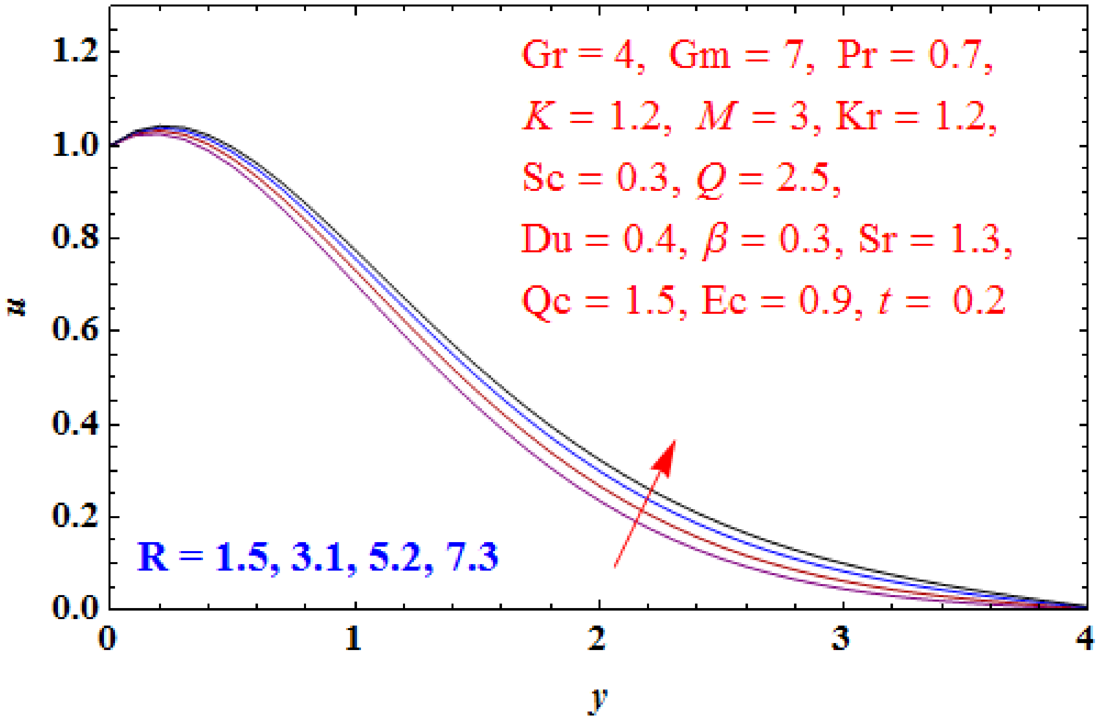

Figure.2 Velocity Profiles for Different Values of R

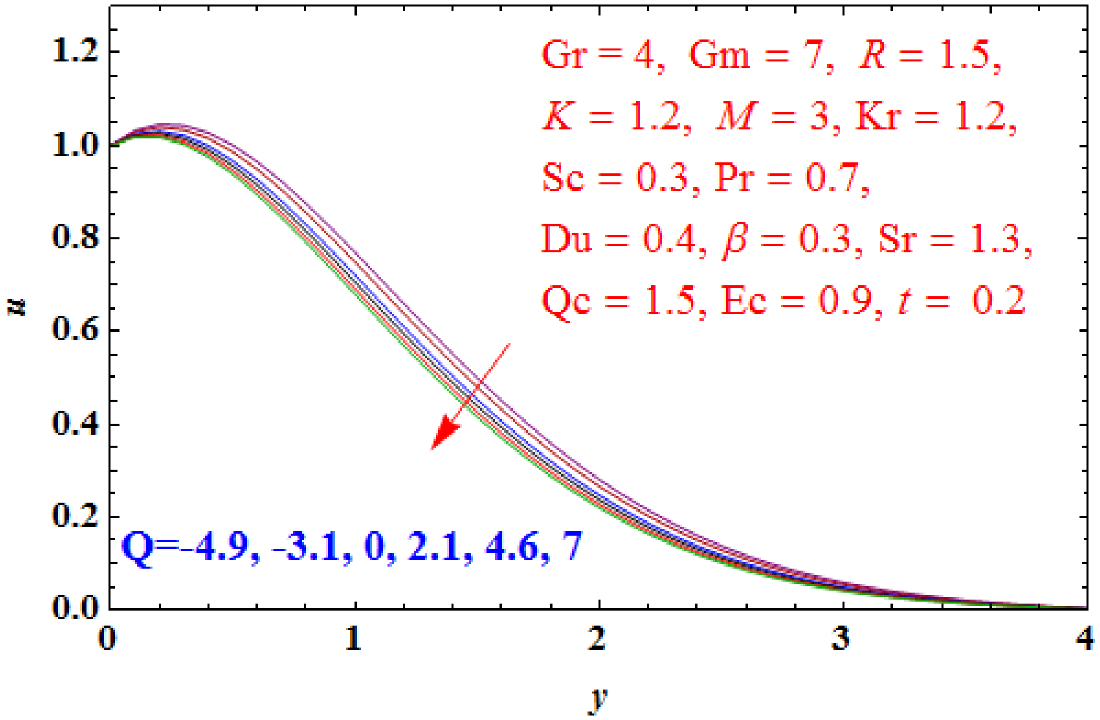

Figure.3 Velocity Profiles for Different Values of Q

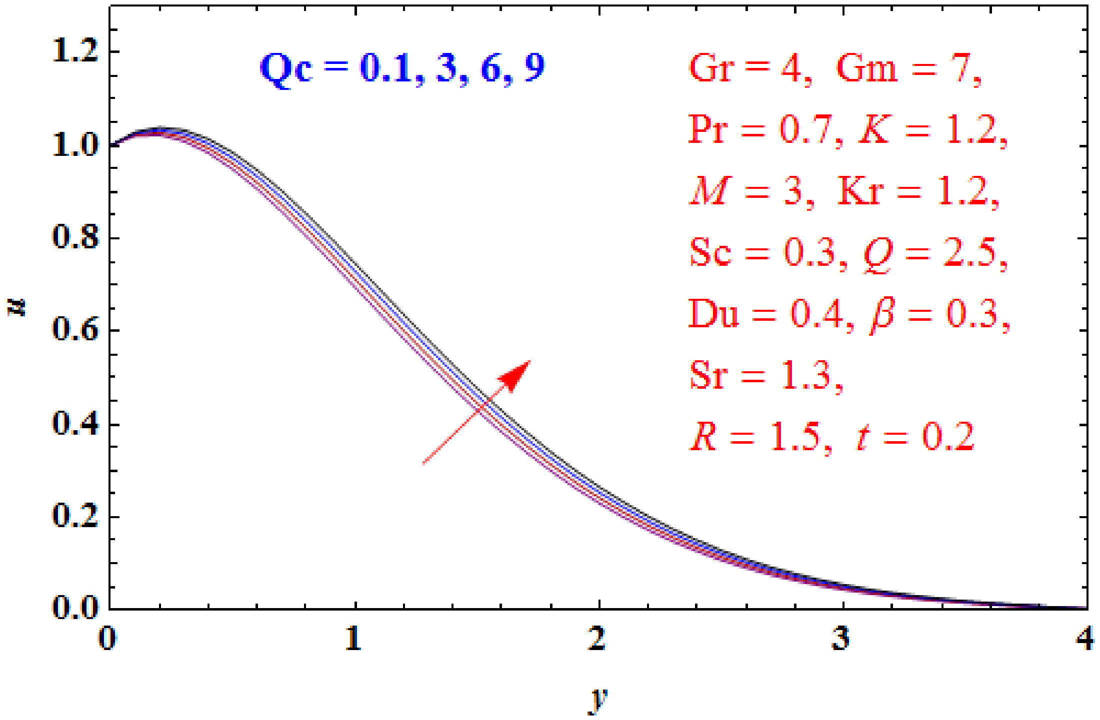

Figure. 4 Velocity Profiles for Different Values of Qc

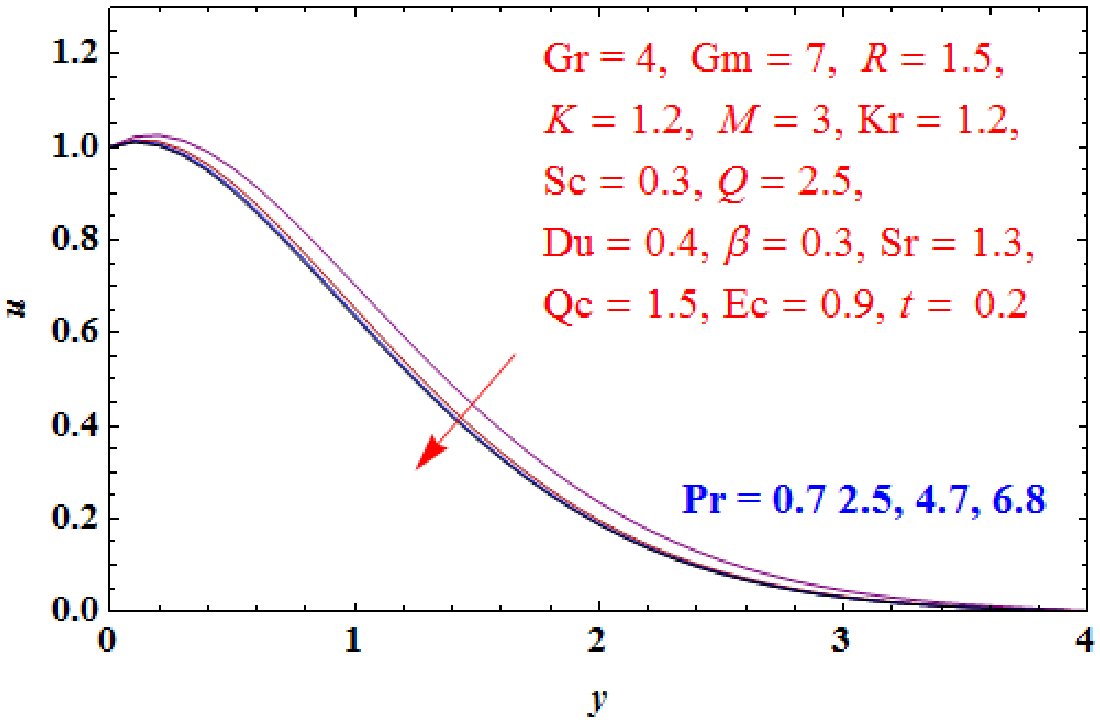

Figure.5 Velocity Profiles for Different Values of Pr

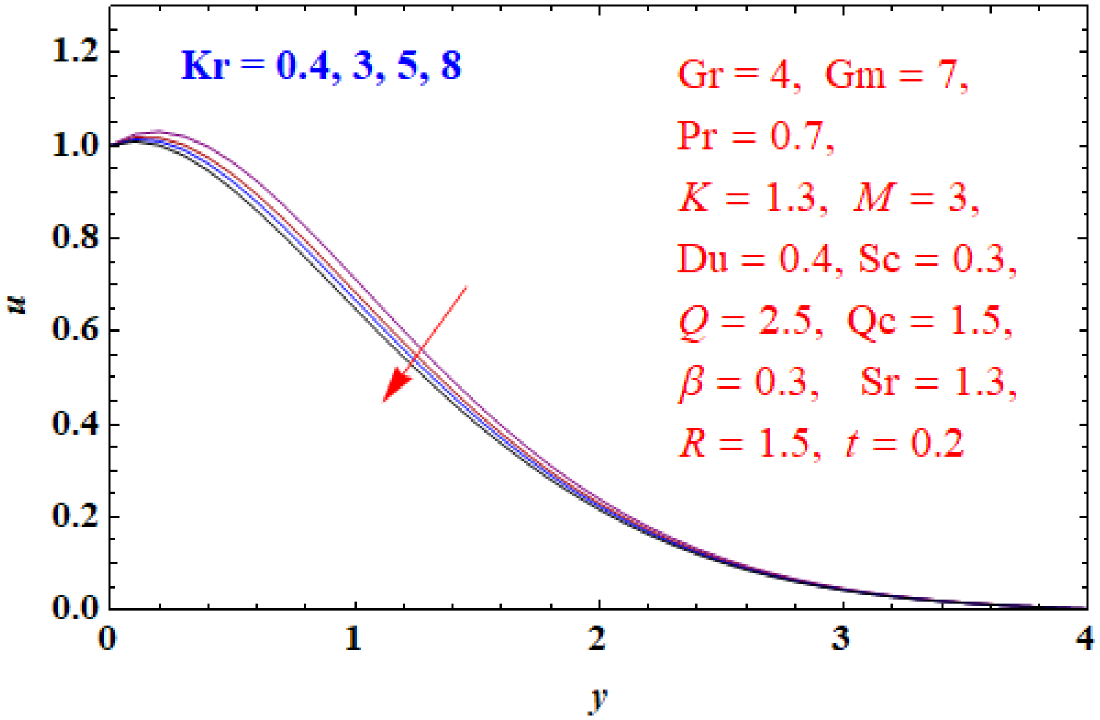

Figure.6 Velocity Profiles for Different Values of Kr

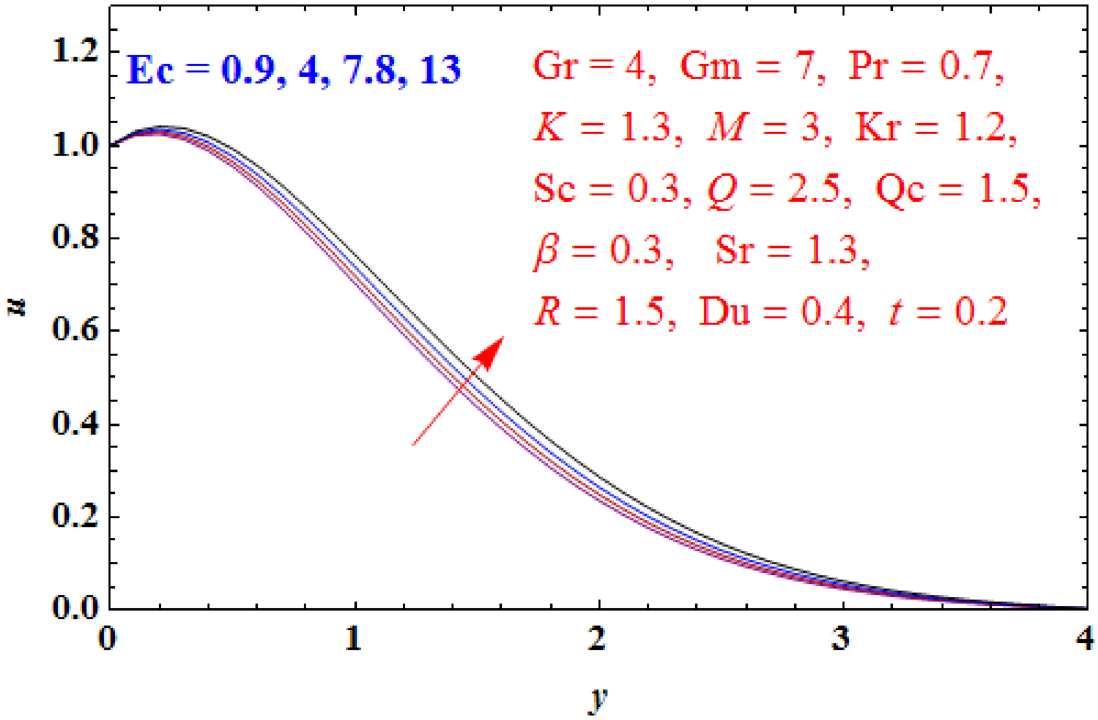

Figure.7 Velocity Profiles for Different Values of Ec

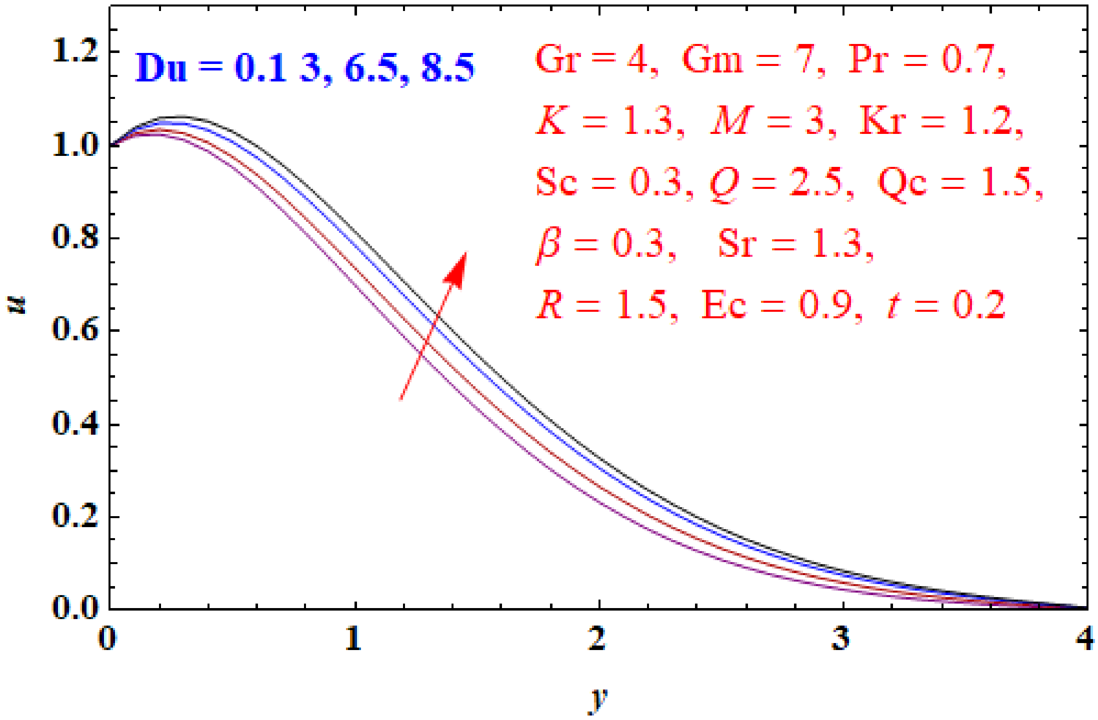

Figure.8 Velocity Profiles for Different Values of Du

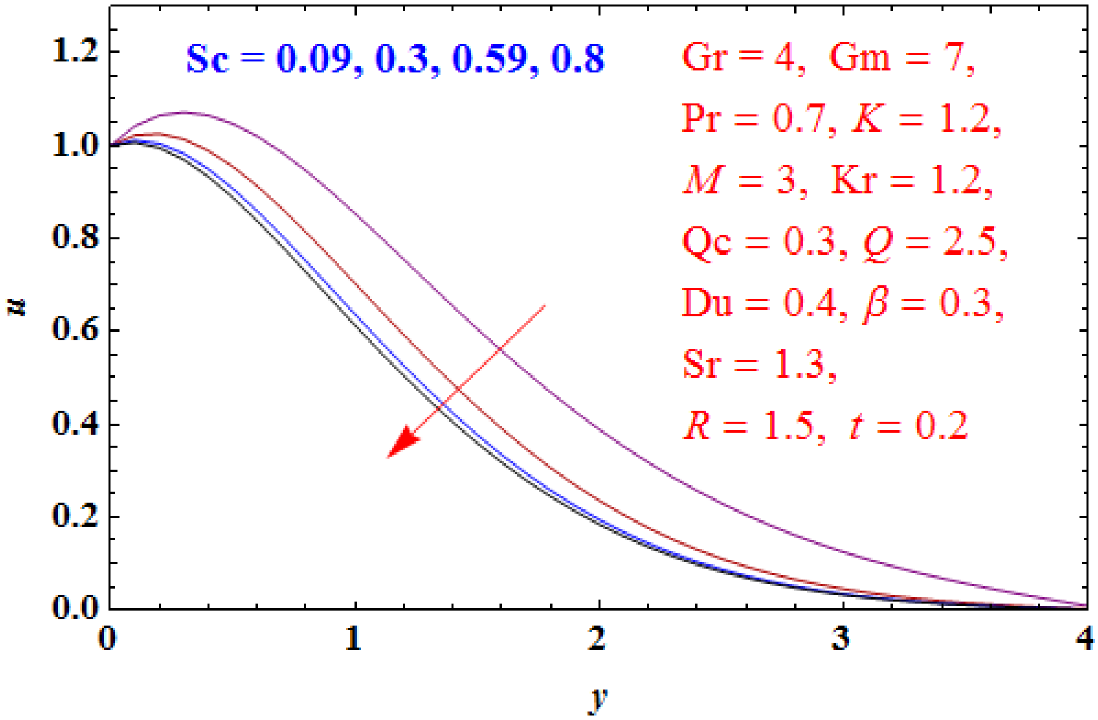

Figure. 9 Velocity Profiles for Different Values of Sc

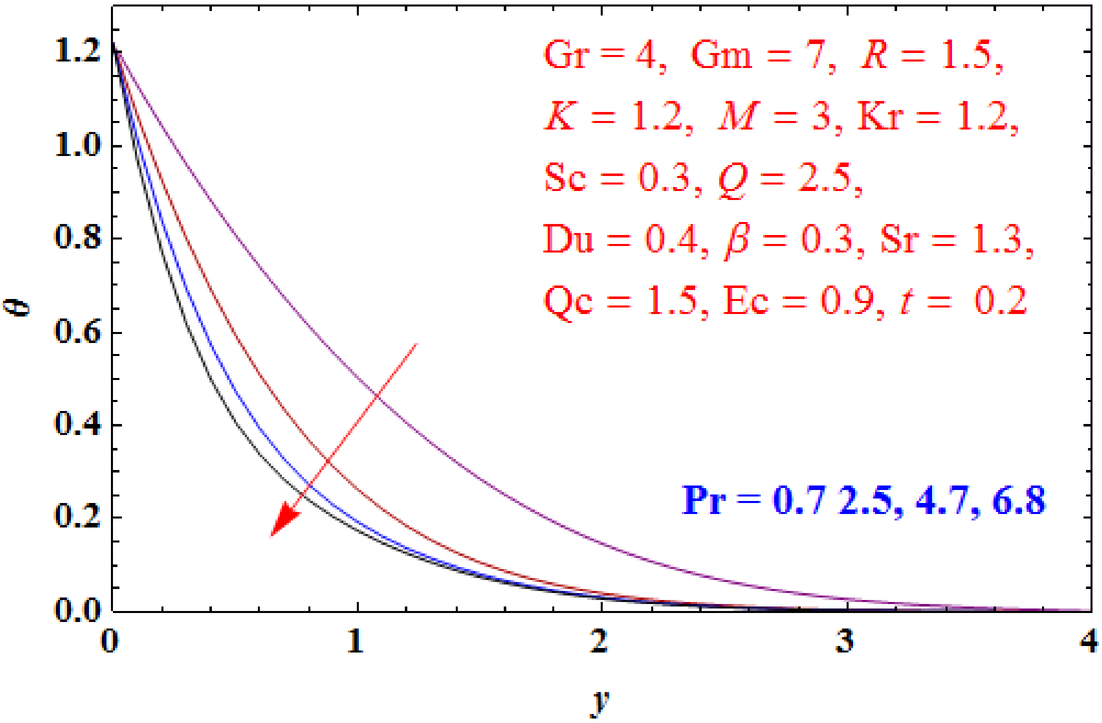

Figure.10 Temperature Profiles for Different Values of Pr

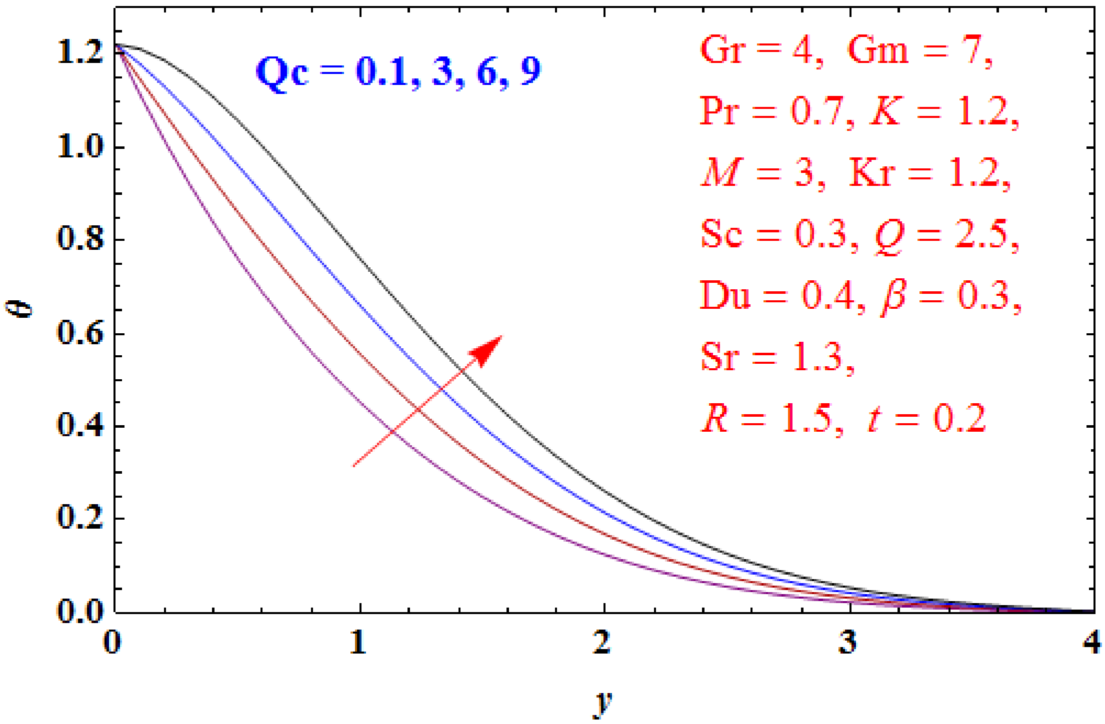

Figure.11 Temperature Profiles for Different Values of Qc

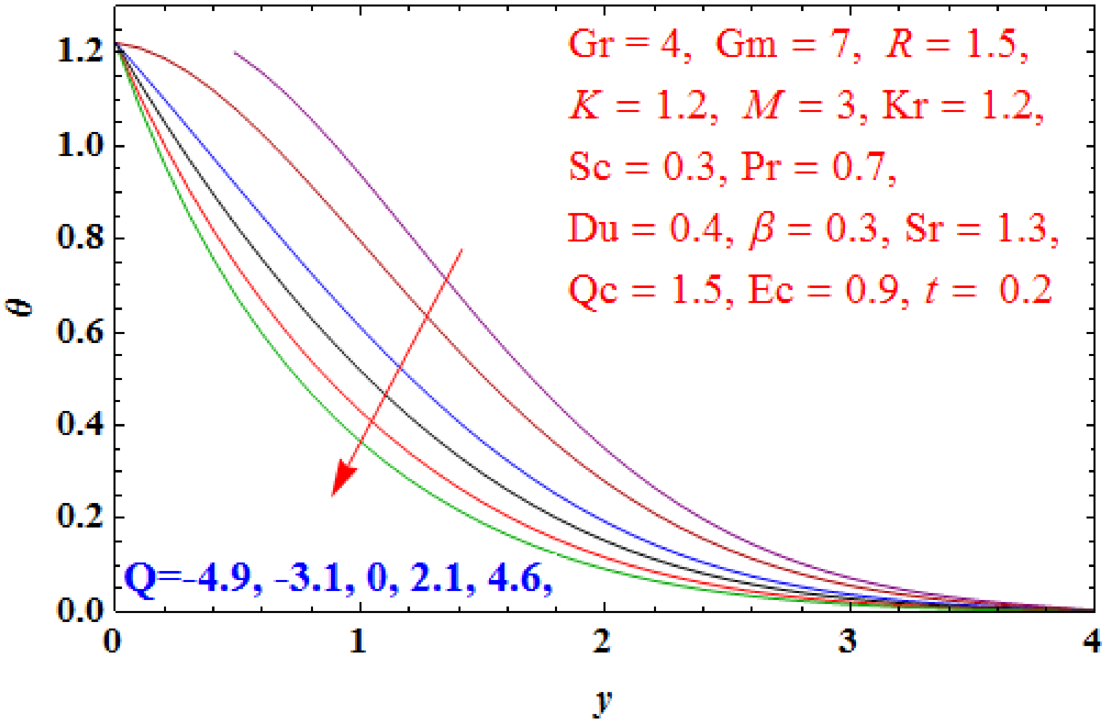

Figure.12 Temperature Profiles for Different Values of Q

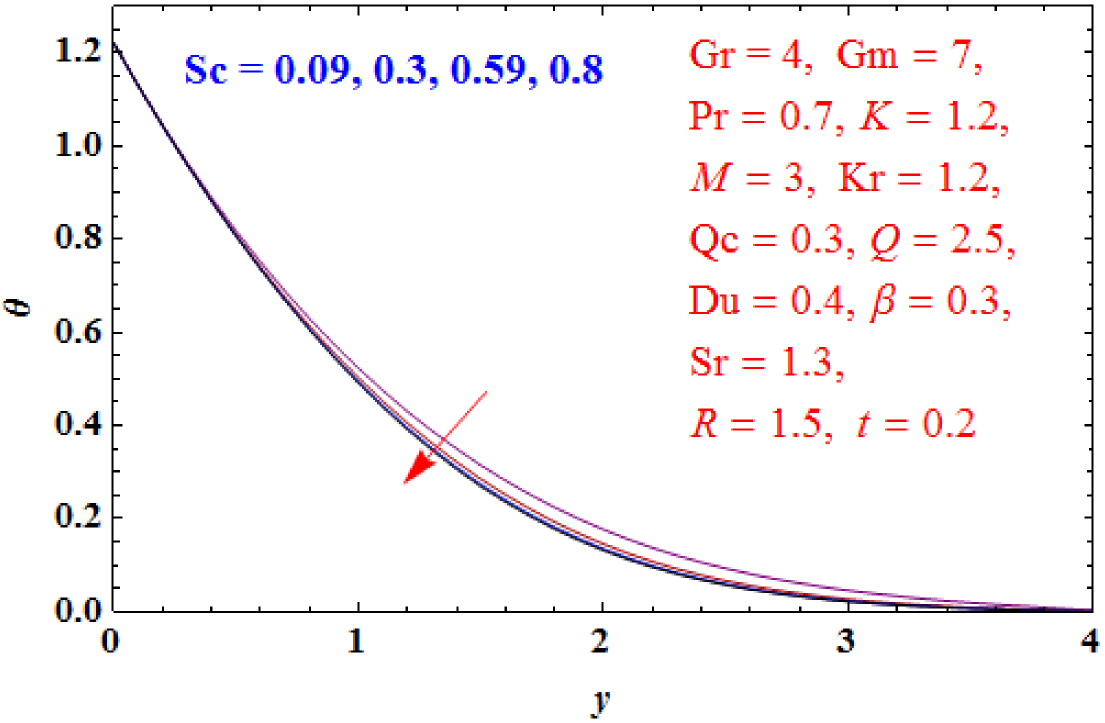

Figure. 13 Temperature Profiles for Different Values of Sc

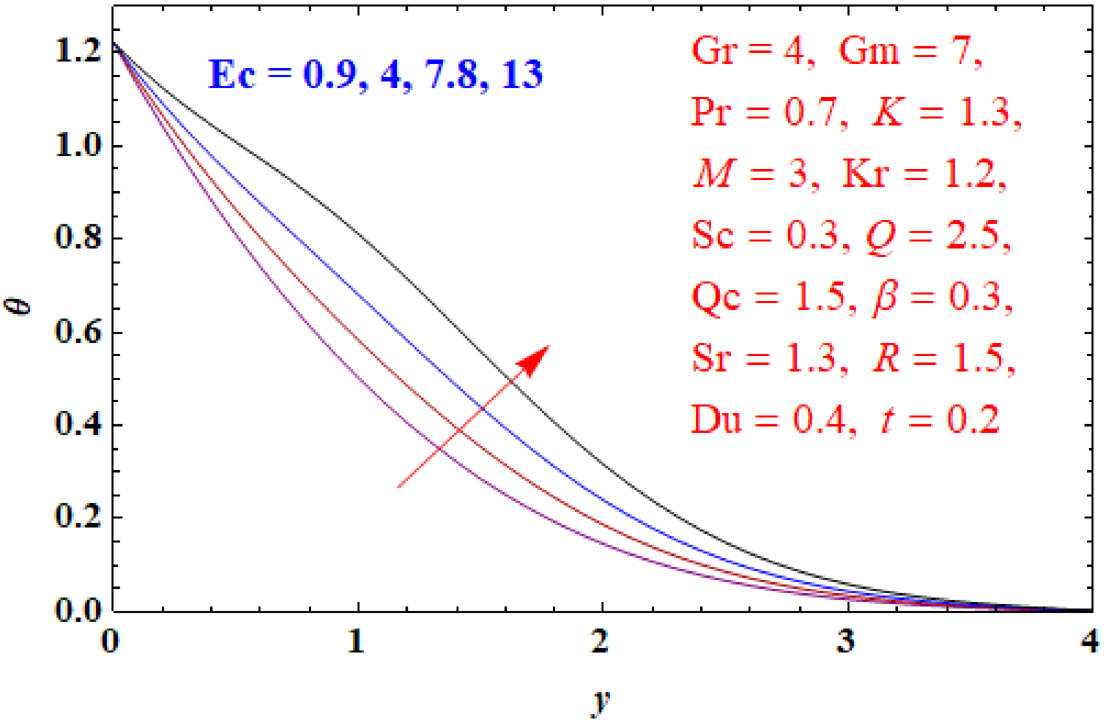

Figure.14 Temperature Profiles for Different Values of Ec

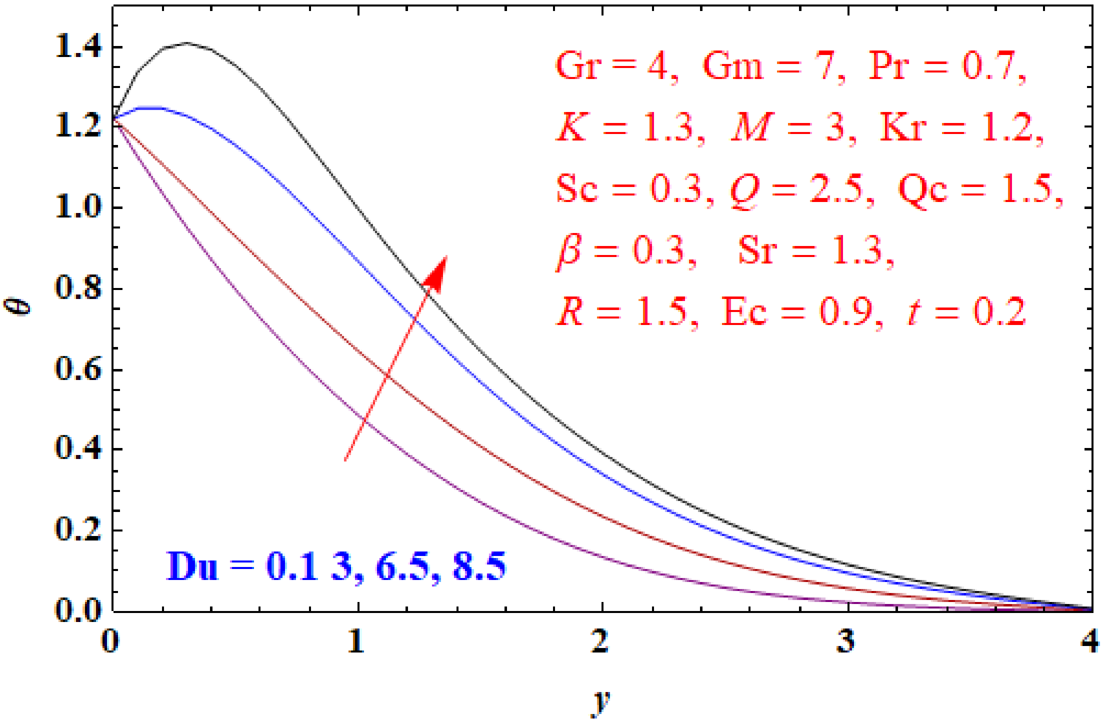

Figure.15 Temperature Profiles for Different Values of Du

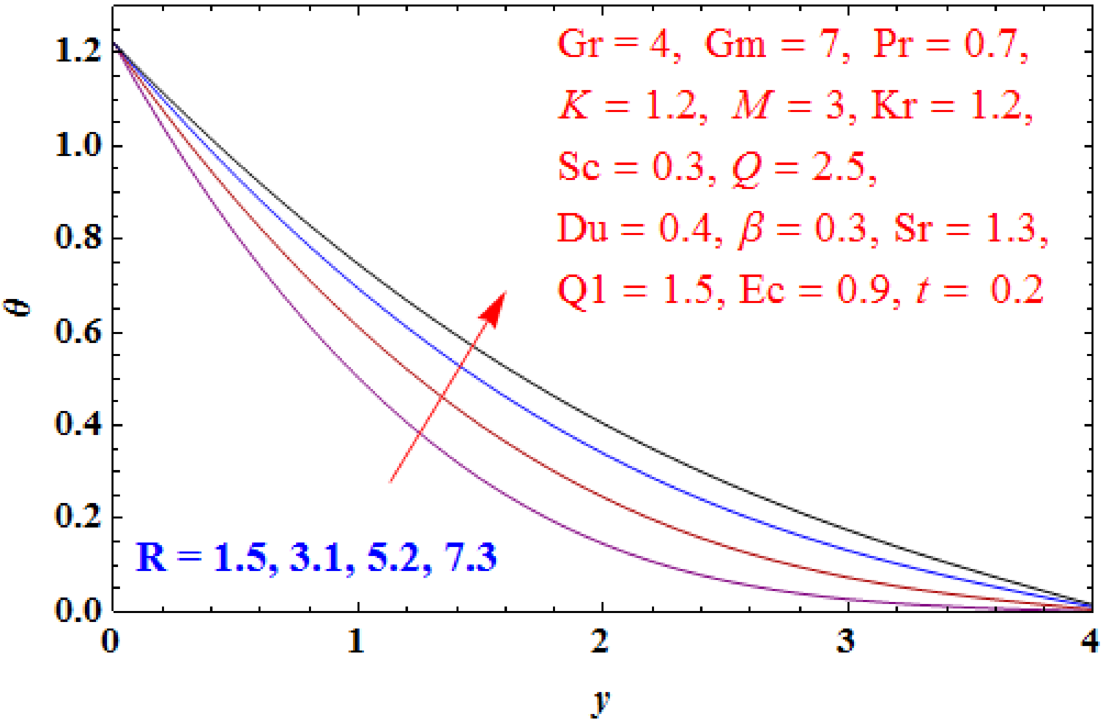

Figure. 16 Temperature Profiles for Different Values of R

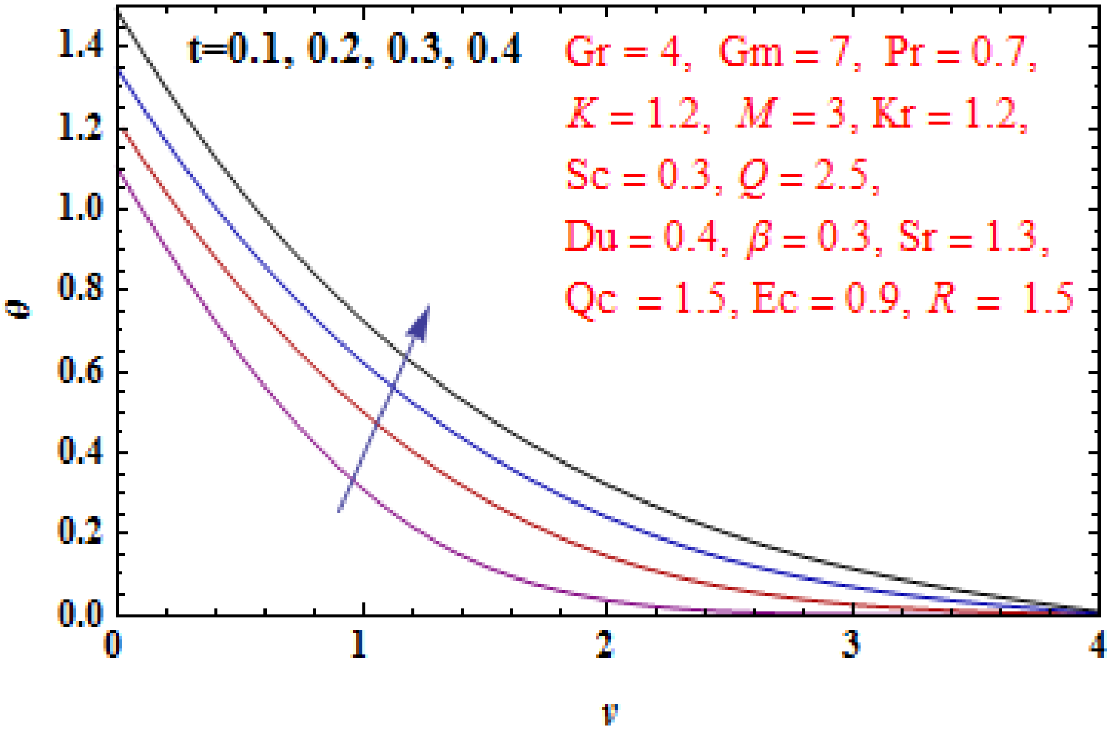

Figure.17 Temperature Profiles for Different Values of t

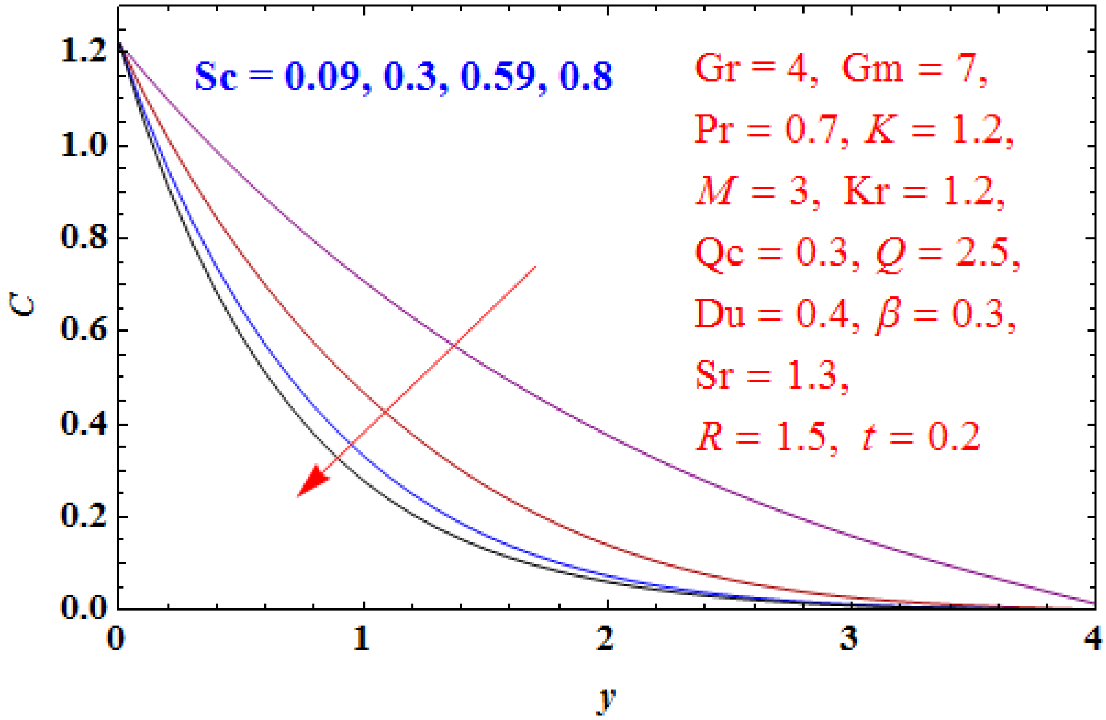

Figure.18 Concentration Profiles for Different Values of Sc

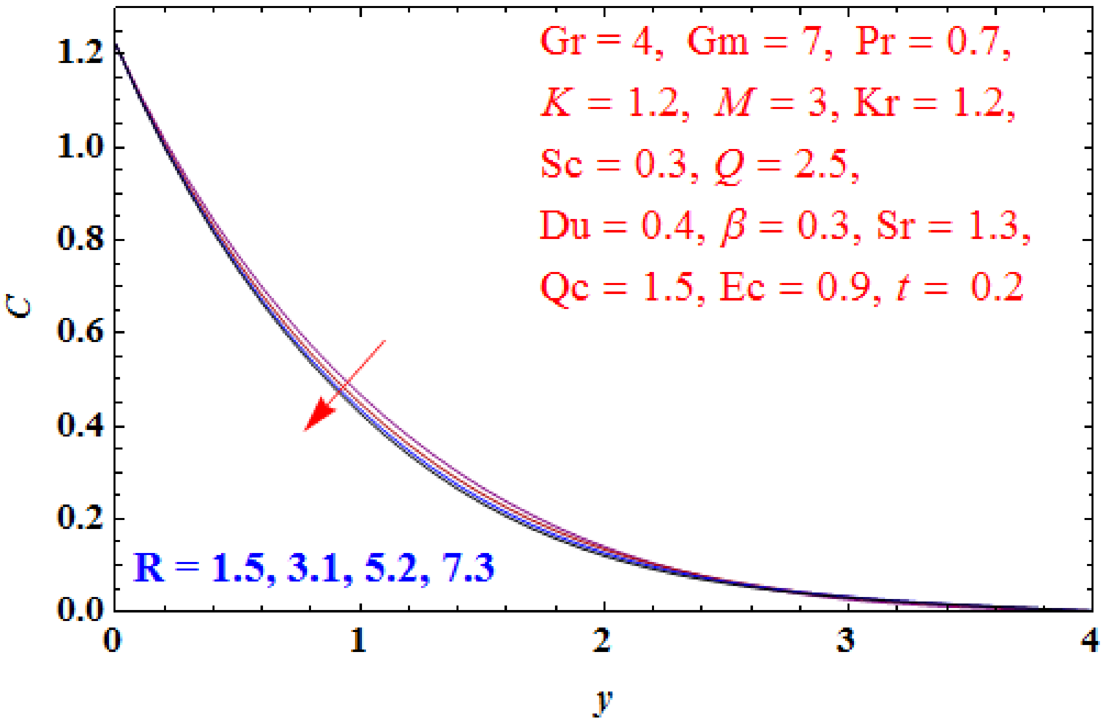

Figure.19 Concentration Profiles for Different Values of R

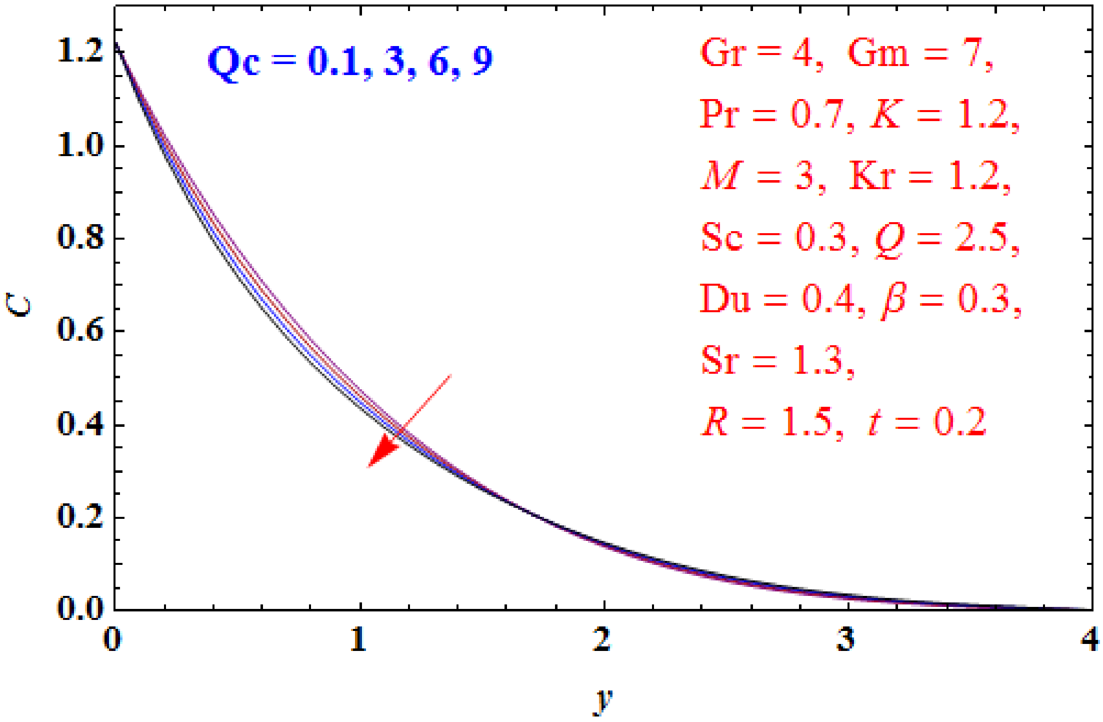

Figure.20 Concentration Profiles for Different Values of Qc

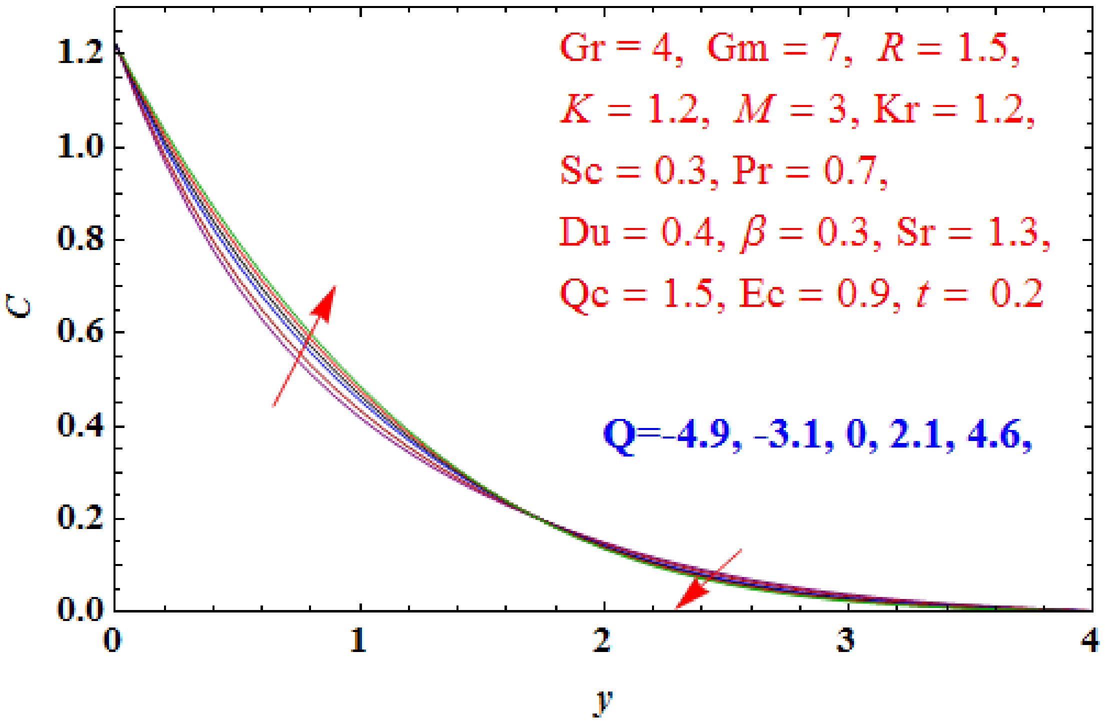

Figure.21 Concentration Profiles for Different Values of Q

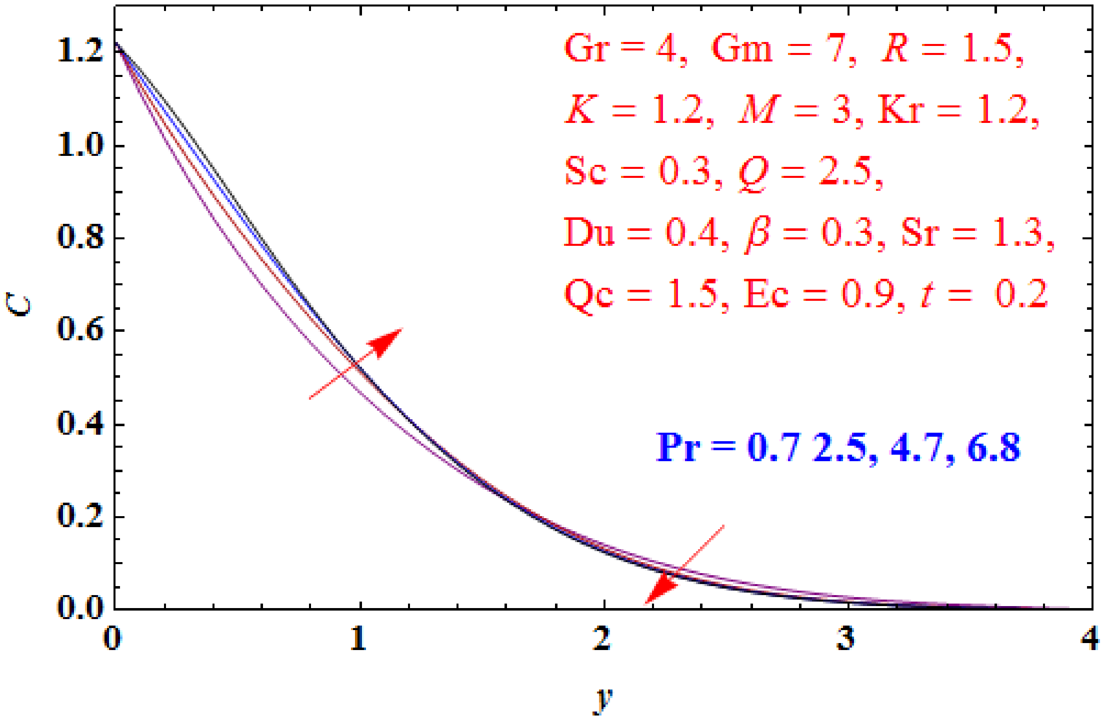

Figure. 22 Concentration Profiles for Different Values of Pr

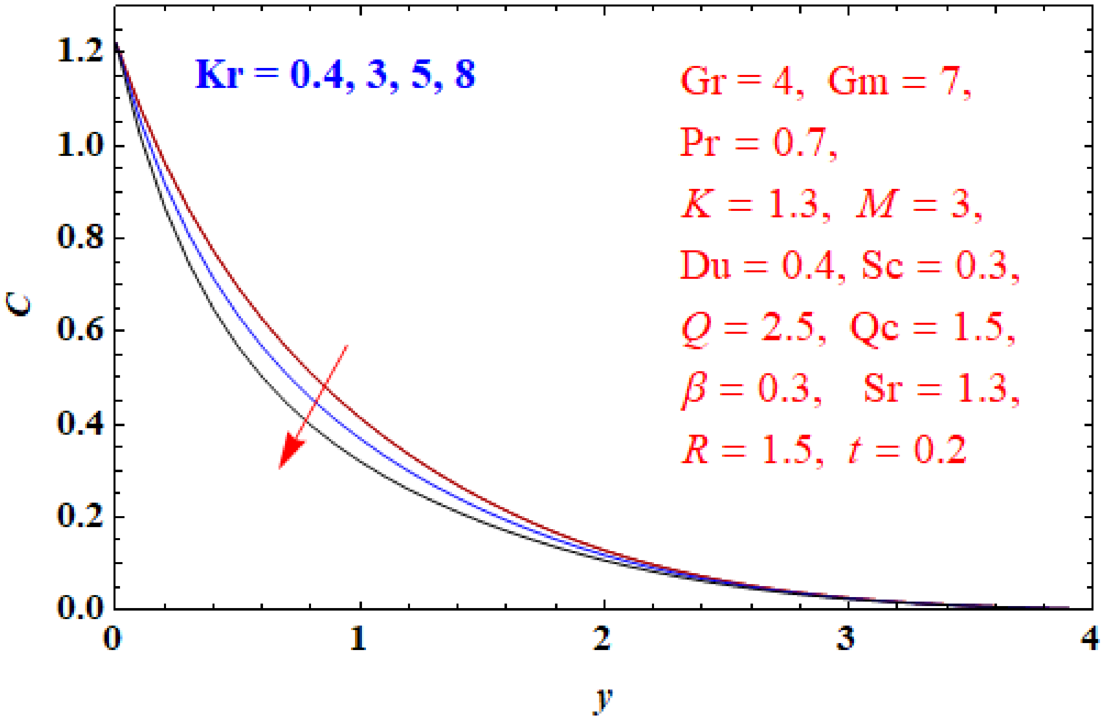

Figure.23 Concentration Profiles for Different Values of Kr

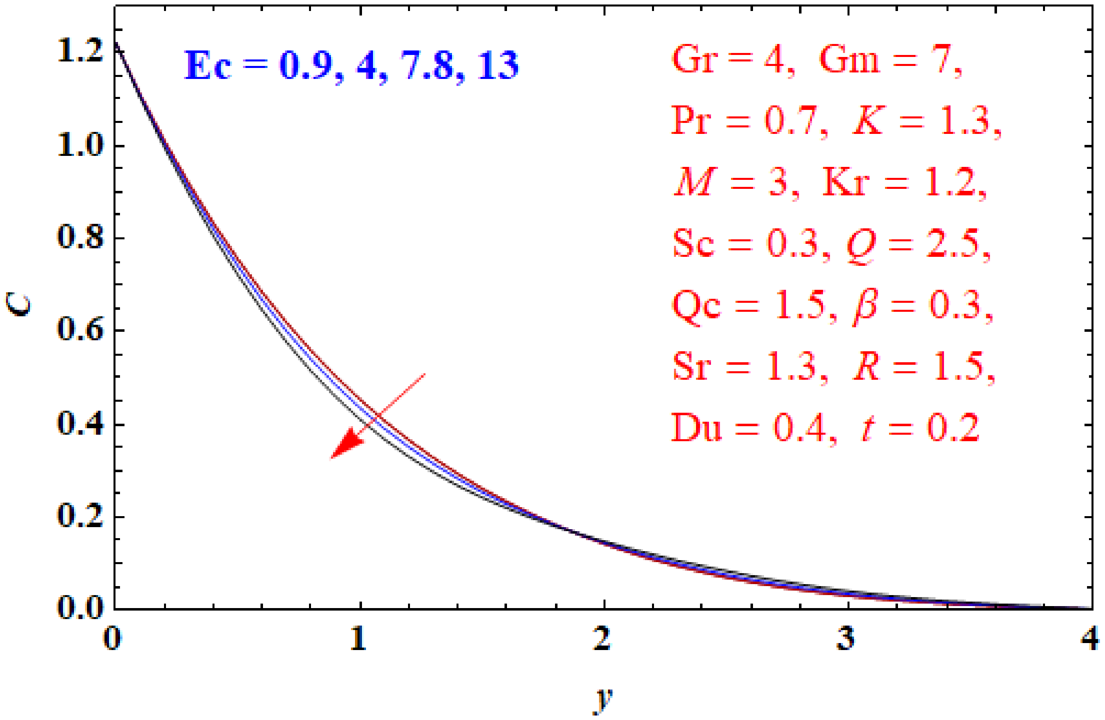

Figure.24 Concentration Profiles for Different Values of Ec

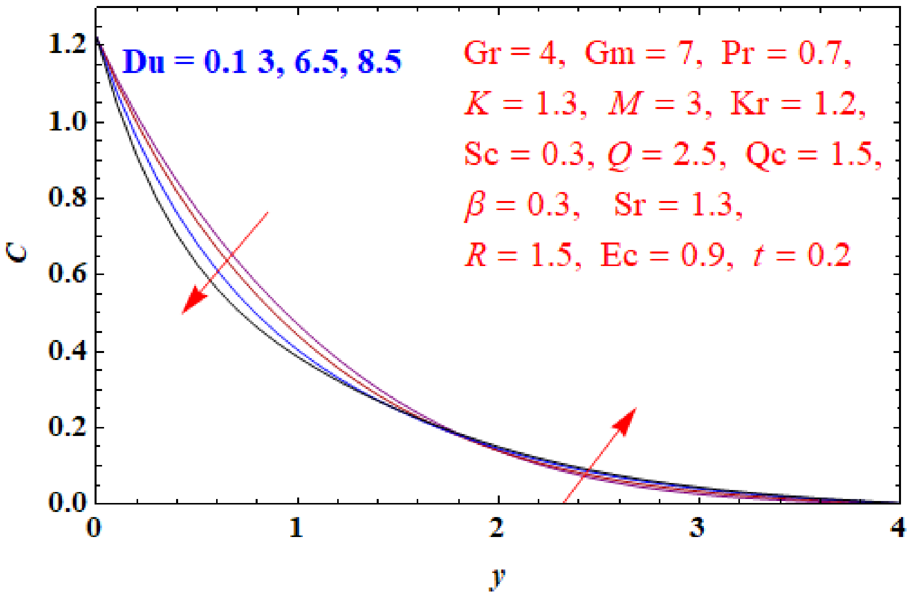

Figure.25 Concentration Profiles for Different Values of Du

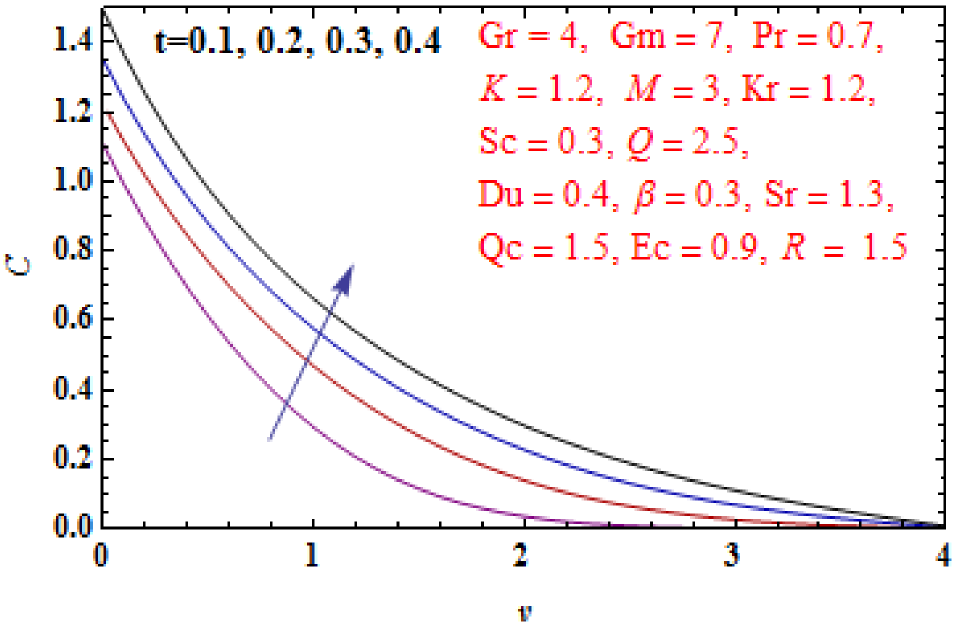

Figure.26 Concentration Profiles for Different Values of t

Table 1.Skin friction coefficient τ, Nusselt number Nu and Sherwood number Sh for different values of parameters taking fix values of Gr = 4, Gm = 7, K = 1.2

β	Du	Kr	Pr	Q	Q_c	S_c	R	S_r	t	Ec	τ	Nu	Sh
0.1	0.4	1.2	0.7	2	1.5	0.3	1.5	1.3	0.2	0.9	0.174425	0.928619	1.07742
1.8	0.4	1.2	0.7	2	1.5	0.3	1.5	1.3	0.2	0.9	-1.16558	0.895153	1.08565
3	0.4	1.2	0.7	2	1.5	0.3	1.5	1.3	0.2	0.9	-1.1464	0.891101	1.08669
5	0.4	1.2	0.7	2	1.5	0.3	1.5	1.3	0.2	0.9	-1.12846	0.888211	1.08743
0.3	**0.1**	1.2	0.7	2	1.5	0.3	1.5	1.3	0.2	0.9	-0.931582	0.951975	1.07092
0.3	**3**	1.2	0.7	2	1.5	0.3	1.5	1.3	0.2	0.9	-1.14836	0.550275	1.18124
0.3	**6.5**	1.2	0.7	2	1.5	0.3	1.5	1.3	0.2	0.9	-1.46338	-0.251386	1.42177
0.3	**8.5**	1.2	0.7	2	1.5	0.3	1.5	1.3	0.2	0.9	-1.69204	-1.16759	1.72165
0.3	0.4	**0.4**	0.7	2	1.5	0.3	1.5	1.3	0.2	0.9	-1.05731	0.923049	0.915066
0.3	0.4	**3**	0.7	2	1.5	0.3	1.5	1.3	0.2	0.9	-0.757126	0.903278	1.39009
0.3	0.4	**5**	0.7	2	1.5	0.3	1.5	1.3	0.2	0.9	-0.58549	0.89083	1.66517
0.3	0.4	**8**	0.7	2	1.5	0.3	1.5	1.3	0.2	0.9	-0.386029	0.874977	1.99275
0.3	0.4	1.2	**0.7**	2	1.5	0.3	1.5	1.3	0.2	0.9	-0.95269	0.916403	1.08037
0.3	0.4	1.2	**2.5**	2	1.5	0.3	1.5	1.3	0.2	0.9	-0.637565	1.56254	0.897232

0.3	0.4	1.2	**4.7**	2	1.5	0.3	1.5	1.3	0.2	0.9	0.118682	2.07928	0.729172
0.3	0.4	1.2	**6.8**	2	1.5	0.3	1.5	1.3	0.2	0.9	0.104214	2.50839	0.581248
0.3	0.4	1.2	0.7	**-4.9**	1.5	0.3	1.5	1.3	0.2	0.9	-1.39973	-0.227826	1.34081
0.3	0.4	1.2	0.7	**-3.1**	1.5	0.3	1.5	1.3	0.2	0.9	-1.26179	0.11357	1.26828
0.3	0.4	1.2	0.7	**0**	1.5	0.3	1.5	1.3	0.2	0.9	-1.07218	0.597497	1.1582
0.3	0.4	1.2	0.7	**2.1**	1.5	0.3	1.5	1.3	0.2	0.9	-0.970166	0.868854	1.09226
0.3	0.4	1.2	0.7	**4.6**	1.5	0.3	1.5	1.3	0.2	0.9	-0.869648	1.1477	1.02106
0.3	0.4	1.2	0.7	**7**	1.5	0.3	1.5	1.3	0.2	0.9	-0.78988	1.38022	0.958897
0.3	0.4	1.2	0.7	2	**0.1**	0.3	1.5	1.3	0.2	0.9	-0.895115	1.07557	1.04018
0.3	0.4	1.2	0.7	2	**3**	0.3	1.5	1.3	0.2	0.9	-1.01355	0.748439	1.12292
0.3	0.4	1.2	0.7	2	**6**	0.3	1.5	1.3	0.2	0.9	-1.13275	0.420298	1.20642
0.3	0.4	1.2	0.7	2	**9**	0.3	1.5	1.3	0.2	0.9	-1.24868	0.102209	1.28785
0.3	0.4	1.2	0.7	2	1.5	**0.09**	1.5	1.3	0.2	0.9	-1.81849	0.905883	0.631943
0.3	0.4	1.2	0.7	2	1.5	**0.3**	1.5	1.3	0.2	0.9	-0.95269	0.916403	1.08037
0.3	0.4	1.2	0.7	2	1.5	**0.59**	1.5	1.3	0.2	0.9	-0.479854	0.91033	1.45625
0.3	0.4	1.2	0.7	2	1.5	**0.8**	1.5	1.3	0.2	0.9	-0.277594	0.903226	1.66762
0.3	0.4	1.2	0.7	2	1.5	0.3	**1.5**	1.3	0.2	0.9	-0.95269	0.916403	1.08037
0.3	0.4	1.2	0.7	2	1.5	0.3	**3.1**	1.3	0.2	0.9	-1.10667	0.732565	1.12351
0.3	0.4	1.2	0.7	2	1.5	0.3	**5.2**	1.3	0.2	0.9	0.28512	0.609872	1.14919
0.3	0.4	1.2	0.7	2	1.5	0.3	**7.3**	1.3	0.2	0.9	0.305612	0.537483	1.16327
0.3	0.4	1.2	0.7	2	1.5	0.3	1.5	**0.1**	0.2	0.9	-0.717839	0.91842	1.20661
0.3	0.4	1.2	0.7	2	1.5	0.3	1.5	**1.3**	0.2	0.9	-0.95269	0.916403	1.08037
0.3	0.4	1.2	0.7	2	1.5	0.3	1.5	**4**	0.2	0.9	-1.4674	0.911631	0.798609
0.3	0.4	1.2	0.7	2	1.5	0.3	1.5	**5.3**	0.2	0.9	-1.70886	0.909237	0.663927
0.3	0.4	1.2	0.7	2	1.5	0.3	1.5	1.3	**0.1**	0.9	1.35398	1.01281	1.15127
0.3	0.4	1.2	0.7	2	1.5	0.3	1.5	1.3	**0.2**	0.9	-0.95269	0.916403	1.08037
0.3	0.4	1.2	0.7	2	1.5	0.3	1.5	1.3	**0.3**	0.9	-2.44239	0.929964	1.14956
0.3	0.4	1.2	0.7	2	1.5	0.3	1.5	1.3	**0.4**	0.9	-3.6763	0.978198	1.27522
0.3	0.4	1.2	0.7	2	1.5	0.3	1.5	1.3	0.2	**0.9**	-0.95269	0.916403	1.08037
0.3	0.4	1.2	0.7	2	1.5	0.3	1.5	1.3	0.2	**4**	-1.04339	0.80389	1.10727
0.3	0.4	1.2	0.7	2	1.5	0.3	1.5	1.3	0.2	**7.8**	-1.15264	0.672945	1.13841
0.3	0.4	1.2	0.7	2	1.5	0.3	1.5	1.3	0.2	**13**	-1.29895	0.504645	1.1782

REFERENCES

[1]. Shafiq A., Rasool G. and Tlili I.(2020),"Marangoni convective nanofluid flow over an electromagnetic actuator in the presence of first-order chemical reaction" Heat Transf. Asian Res /Vol.49/ Pp. 274–288.

[2]. Parvin S.; Mohamed Isa S.S.P., Arifin, N.M., Md Ali, F.(2021),"The Inclined Factors of Magnetic Field and Shrinking Sheet in Casson Fluid Flow, Heat and Mass TransferSymmetry"/Vol.13/ No.373, https://doi.org/10.3390/ sym13030373.

[3]. Lahmar Sihem, Kezzar Mohamed, Eid Mohamed R., and Sari, Mohamed Rafik (2020),"Heat transfer of squeezing unsteady nanofluid flow under the effects of an inclined magnetic field and variable thermal conductivity" Physica A: Statistical Mechanics and its Applications, Elsevier / Vol. 540(C).

[4]. M. R. Eid, K. Mahny, A. Dar and T. Muhammad (2020),"Numerical study for Carreau nanofluid flow over aconvectively heated nonlinear stretching surface with chemically reactive species" Physica A: Statistical Mechanics and Its Applications /Vol. 540/ 123063.

[5]. Hammad Alotaibi, Saeed Althubiti, Mohamed R. Eid, K. L. Mahny (2021),"Numerical Treatment of MHD Flow of Casson Nanofluid via Convectively Heated Non-Linear Extending Surface with Viscous Dissipation and Suction/Injection Effects"/Vol. 66/ No.1, Pp. 229-245, doi:10.32604/cmc.2020.012234.

[6]. K. K. Asogwa and A. A. Ibe, (2020),"A Study of MHD Casson Fluid Flow over a Permeable Stretching Sheet with Heat and Mass Transfer" Journal of Engineering Research and Reports /Vol. 16/ No.2, Pp. 10-25.

[7]. Renu Devi, Vikas Poply, Manimala (2021),"Effect of aligned magnetic field and inclined outer velocity in casson fluid flow over a stretching sheet with heat source" Journal of Thermal Engineering /Vol.7/ No.4, Pp. 823-844.

[8]. K Kumar Anantha, , Ankalagiri Ramudu Sugunamma Vangala, Dr.N. Sandeep (2021),"Impact of Soret and Dufour on MHD Casson fluid flow past a stretching surface with convective-diffusive conditions" Journal of Thermal Analysis and Calorimetry 10.1007/s10973-021-10569-w.

[9]. U. S. Mahabaleshwar, K. N. Sneha, Akio Miyara, M. Hatami (2022),"Radiation effect on inclined MHD flow past a super-linear stretching/shrinking sheet including CNTs, Waves in Random and Complex Media" DOI: 10.1080/17455030.2022.2053238.

[10]. Ram Prakash Sharma and Sachin Shaw (2022),"MHD Non-Newtonian Fluid Flow past a Stretching Sheet under the Influence of Non-linear Radiation and Viscous Dissipation"J. Appl. Comput. Mech. /Vol. 8/ No. 3, Pp. 949-961.

[11]. Naveed Akbar, Sardar Muhammad Hussain and Riaz Ullah Khan (2022),"Numerical Solution of Casson Fluid Flow under Viscous Dissipation and Radiation Phenomenon" Journal of Applied Mathematics and Physics /Vol. 10/ Pp. 475-490.

[12]. Elham Alali Elham Alali and Ahmed M. Megahed (2022),"MHD dissipative Casson nanofluid liquid film flow due to an unsteady stretching sheet with radiation influence and slip velocity phenomenon" Nanotechnology Reviews/ Vol. 11/ Pp. 463–472

[13]. T. M. Ajayi, A. J. Omowaye, and I. L. Animasaun(2017), "Viscous Dissipation Effects on the Motion of Casson Fluid over an Upper Horizontal Thermally Stratified Melting Surface of a Paraboloid of Revolution: Boundary Layer Analysis" Hindawi Journal of Applied Mathematics /Vol. 2017/ https://doi.org/10.1155/2017/1697135.

[14]. N. Pandya and A. K. Shukla (2014),"Effects of Thermophoresis, Dufour, Hall and Radiation on an Unsteady MHD flow past an Inclined Plate with Viscous Dissipation"International Journal of Mathematics and Scientific Computing /Vol. 4/ No.2.

[15]. Brice Carnahan, H.A. Luther and James O. Wilkes. (1990), Applied Numerical Methods, Krieger Pub Co, Florida.

[16]. T. G. Cowling (1990), Magneto-Hydrodynamics, Inter Science Publishers, New York**.**